British Journal of Pharmacology

DOI:10.1111/j.1476-5381.2012.02126.x
www.brjpharmacol.org

RESEARCH PAPER

Novel pyrazole compounds for pharmacological discrimination between receptor-operated and store-operated Ca^{2+} entry pathways

H Schleifer[1], B Doleschal[2], M Lichtenegger[2], R Oppenrieder[2], I Derler[3], I Frischauf[3], TN Glasnov[4], CO Kappe[4], C Romanin[3] and K Groschner[1,2]*

[1]*Institute of Biophysics, Medical University of Graz, Graz, Austria,* [2]*Institute of Pharmaceutical Sciences, Department of Pharmacology and Toxicology, University of Graz, Graz, Austria,* [3]*Institute for Biophysics, University of Linz, Linz, Austria, and* [4]*Christian Doppler Laboratory for Microwave Chemistry, Institute of Chemistry, University of Graz, Graz, Austria*

Correspondence
Dr Klaus Groschner, Medical University of Graz, Institute of Biophysics, Harrachgasse 21/IV, 8010 Graz, Austria. E-mail: klaus.groschner@medunigraz.at

Keywords
pyrazole Ca^{2+} channel blockers; transient receptor potential; Orai; store-operated Ca^{2+} entry; receptor operated Ca^{2+} entry; NFAT signalling; mast cell degranulation

Received
31 January 2012
Revised
4 July 2012
Accepted
11 July 2012

BACKGROUND AND PURPOSE

Pyrazole derivatives have recently been suggested as selective blockers of transient receptor potential cation (TRPC) channels but their ability to distinguish between the TRPC and Orai pore complexes is ill-defined. This study was designed to characterize a series of pyrazole derivatives in terms of TRPC/Orai selectivity and to delineate consequences of selective suppression of these pathways for mast cell activation.

EXPERIMENTAL APPROACH

Pyrazoles were generated by microwave-assisted synthesis and tested for effects on Ca^{2+} entry by Fura-2 imaging and membrane currents by patch-clamp recording. Experiments were performed in HEK293 cells overexpressing TRPC3 and in RBL-2H3 mast cells, which express classical store-operated Ca^{2+} entry mediated by Orai channels. The consequences of inhibitory effects on Ca^{2+} signalling in RBL-2H3 cells were investigated at the level of both degranulation and nuclear factor of activated T-cells activation.

KEY RESULTS

Pyr3, a previously suggested selective inhibitor of TRPC3, inhibited Orai1- and TRPC3-mediated Ca^{2+} entry and currents as well as mast cell activation with similar potency. By contrast, Pyr6 exhibited a 37-fold higher potency to inhibit Orai1-mediated Ca^{2+} entry as compared with TRPC3-mediated Ca^{2+} entry and potently suppressed mast cell activation. The novel pyrazole Pyr10 displayed substantial selectivity for TRPC3-mediated responses (18-fold) and the selective block of TRPC3 channels by Pyr10 barely affected mast cell activation.

CONCLUSIONS AND IMPLICATIONS

The pyrazole derivatives Pyr6 and Pyr10 are able to distinguish between TRPC and Orai-mediated Ca^{2+} entry and may serve as useful tools for the analysis of cellular functions of the underlying Ca^{2+} channels.

Abbreviations

BTP, 3,5-bis(trifluoromethyl)pyrazole derivative; CRAC, Ca^{2+} release activated current; DAG, diacylglycerol; ER, endoplasmatic reticulum; NFAT, nuclear factor of activated T-cells; OAG, 1-oleoyl-2-acetyl-sn-glycerol; OM, orders of magnitude; ROCE, receptor operated Ca^{2+} entry; SOCE, store-operated Ca^{2+} entry; STIM1, stromal interaction molecule 1; TRPC channel, transient receptor potential canonical channel

Introduction

Changes in cytosolic Ca^{2+} concentration control a broad range of cell- and tissue-specific processes reaching from B-cell activation, mast cell degranulation and cardiac pathologies, to cell proliferation and gene expression. Ca^{2+} entry via plasma membrane channels can be mediated by a diverse array of extra- and intracellular stimuli (Berridge *et al.*, 2000). Characterization of the mechanisms that govern Ca^{2+} channel function has resulted in a commonly accepted distinction between 'receptor operated Ca^{2+} entry' (ROCE) pathways that take place in response to receptor agonist/ligand-induced phospholipase C-mediated phosphoinositol-4,5-bisphosphate hydrolysis formation (Hofmann *et al.*, 1999; Lemonnier *et al.*, 2008) and 'store operated Ca^{2+} entry' (SOCE), which is activated as a consequence of depletion of endoplasmic reticulum (ER) Ca^{2+} stores. Until the discovery of stromal interaction molecule 1 (STIM1) and Orai1 as key components of the latter process (Zhang *et al.*, 2005; Prakriya *et al.*, 2006), the family of canonical transient receptor potential channels (TRPCs) (Pedersen *et al.*, 2005; Nilius *et al.*, 2007; Abramowitz and Birnbaumer, 2009) has been considered the prime candidates for both Ca^{2+} entry pathways. Due to inherent overlap and crosstalk of the two mechanisms as well as the paucity of model systems that unequivocally lack one of these components, a clear-cut distinction between Orai1-meditated SOCE and TRPC-mediated ROCE appears difficult. Moreover, physical interactions between these two channel proteins in either a direct or indirect way has been proposed (Liao *et al.*, 2007; Jardin *et al.*, 2008; Yuan *et al.*, 2009; Woodard *et al.*, 2010; Cheng *et al.*, 2011), and both Ca^{2+} influx pathways are tightly linked to downstream gene transcription via nuclear factor of activated T-cells (NFAT) (Sinkins *et al.*, 2004; Kar *et al.*, 2011).

Therefore, specific and potent pharmacological tools are highly desirable for further analysis of the contribution of either protein species or Ca^{2+} channel complexes to Ca^{2+} signalling and downstream cellular events. Inorganic blockers like Gd^{3+} or La^{3+} had been used extensively for this purpose as they are considered to interact specifically with TRPC channel pores (Trebak *et al.*, 2002). Similarly, organic compounds such as SKF-96365 (Harteneck and Gollasch, 2011), 2-APB (DeHaven *et al.*, 2008) and SK66 (Ng *et al.*, 2008) have also been used due to their blocking effects on TRPC channels and store-operated Ca^{2+} conductance, with half-maximal concentrations in the low to intermediate micromolar range. All these pharmacological tools share common drawbacks in terms of lacking specificity for blocking a certain Ca^{2+} entry channel. The blockers not only lack selectivity for subtypes of TRPC channels (Harteneck and Gollasch, 2011), but exert, in addition, complex effects on Ca^{2+} entry and currents mediated by the STIM1/Orai1 SOCE pathway (DeHaven *et al.*, 2008).

3,5-Bis(trifluoromethyl)pyrazole derivatives (BTPs), specifcally BTP2/Pyr2, have been proposed as potent small molecule inhibitors of both SOCE and TRPC-mediated ROCE (Zitt *et al.*, 2004; He *et al.*, 2005). Historically, this tool evolved from a class of immunosuppressants analogous to cyclosporine A or so called '-limus drugs' such as sirolimus and tacrolimus (FK506) (Djuric *et al.*, 2000; Chen *et al.*, 2002; Ishikawa *et al.*, 2003). Although primarily affecting NFAT activation and as a consequence cytokine production in immune cells, experiments showed that BTPs are capable of blocking store depletion-activated Ca^{2+} entry into a wide variety of cells at nanomolar to low micromolar concentrations with appreciable selectivity over voltage-gated Ca^{2+} entry. For a general review on BTPs as SOCE blockers, see Sweeney *et al.* (2009).

Recently, Pyr3, a pyrazole derivate, has been proposed as a highly subtype-specific inhibitor of TRPC3 activity (Kiyonaka *et al.*, 2009). Specificity over other TRPC family members and other TRP subtypes in transfected HEK293 cells has been clearly demonstrated and the tricholoroarylic amide bond-linked side group was identified as essential for this property. Moreover, electron drawing side groups in C3 position of the pyrazole ring of BTP and Pyrs were proposed as key structural determinants of the inhibitory effect (Law *et al.*, 2011). Studies demonstrating BTP2/Pyr2 as an inhibitor of receptor-operated TRPC functions, thus lacking selectivity for SOCE (He *et al.*, 2005) and, in turn, Pyr3 as a potent inhibitor of SOCE (Salmon and Ahluwalia, 2010; Kim *et al.*, 2011) have raised doubts about the suitability of these compounds for pharmacological differentiation of these Ca^{2+} entry mechanisms and support the hypothesis of a substantial overlap of these pathways and/or contribution of TRPC3 to SOCE. Applying a recently published synthesis strategy to generate pyrazole derivatives (Obermayer *et al.*, 2011), we characterized the selectivity of four pyrazole compounds, including a new structure, designated as Pyr10, in cell systems that express high levels of well-characterized receptor-operated or store-operated Ca^{2+} channels. We employed HEK293 cells overexpressing TRPC3 as a ROCE model and native RBL-2H3 mast cells as an established Orai-mediated SOCE model (Di Capite and Parekh, 2009).

Our results demonstrate the ability of two pyrazole derivatives to discriminate between the classical Orai-mediated, highly Ca^{2+} selective signalling pathway and the phospholipase C-dependent Ca^{2+} entry-mediated by TRPC channels, specifically by TRPC3. We present Pyr6 and Pyr10 as valuable tools to dissect these signalling pathways.

Methods

DNA, cell culture and transfection

RBL-2H3 and HEK293 cells were cultivated in DMEM medium (Invitrogen, LifeTechnologies, Vienna, Austria) supplemented with 10% FBS. HEK293 cells seeded out in adequate density were transiently transfected by lipofection using FuGENE® (Roche, Vienna, Austria) according to manufacturer's protocol with an n-terminally YFP-tagged TRPC3 cDNA clone to be used as ROCE model or with a CFP-tagged STIM1 and YFP-tagged Orai1 clone to reconstitute the Ca^{2+} release-activated current (CRAC) pore in HEK293 cells (Muik *et al.*, 2008). For NFAT translocation experiments, RBL-2H3 cells were electroporated with a GFP-tagged NFAT construct (at 300 V and 275 μF) with 20 μg of DNA 12–18 h before and seeded out on glass coverslips. For characterization of Pyr6 and Pyr10 selectivity for TRPC channels, n-terminally GFP-tagged murine TRPC6, n-terminally YFP-tagged TRPC5 (Schindl *et al.*, 2008) and c-terminally YFP-tagged TRPC4beta

(Graziani *et al.*, 2010) were used. Detailed procedures and TRPC3 and NFAT constructs have been described previously (Poteser *et al.*, 2011).

All measurements were performed at room temperature.

Reagents and synthesis of pyrazole compounds

If not mentioned otherwise, chemicals were purchased from Sigma Aldrich (Vienna, Austria). For synthesis of the pyrazole compounds, a recently published, optimized three-step microwave procedure was used (Glasnov *et al.*, 2009; Obermayer *et al.*, 2011). In a standard cyclocondensation reaction between 4-nitrophenylhydrazine hydrochloride and corresponding enone or 1,3-dicarbonyl compound under acidic conditions, the desired 1-(4-nitrophenyl)-1H-pyrazoles could be obtained within a short reaction time using microwave heating (160°C, 5 min). The latter products are further reduced into the corresponding anilines in a catalytic transfer hydrogenation procedure with cyclohexene as hydrogen donor over Pd/C (160°C, 2–5 min reaction time). To generate the final Pyr-compounds, two straightforward synthetic routes were available – reaction with an acid in the presence of PCl_3 to conveniently obtain amide-bond derivatives Pyr2, Pyr3 and Pyr6 (150°C, 5 min microwave heating), or reaction with corresponding sulfonyl chlorides in the presence of pyridine as a base (100°C, 5 min microwave heating) to obtain Pyr10. Molecular properties of the compounds were calculated using Molinspiration Property Calculation Service (http://www.molinspiration.com).

Electrophysiology

Patch pipettes were pulled from borosilicate glass capillaries (Harvard Apparatus, Hugo Sachs, March-Hugstetten, Germany; resistance 3–5 MΩ). Currents were recorded at room temperature using a List EPC7 patch-clamp amplifier (HEKA Instruments, Lambrecht, Germany). Signals were low-pass filtered at 3 and 10 kHz and digitized with 5 kHz. For HEK293 cells, voltage-clamp protocols (voltage ramps from –130 to +80 mV, holding potential 0 mV) were controlled by pClamp software (Axon Instruments, Molecular Devices, Biberach, Germany). Extracellular solution (ECS) contained (in mM) 140 NaCl, 2 $CaCl_2$, 2 $MgCl_2$, 10 glucose, pH adjusted to 7.4 with NaOH. The pipette solution (ICS) contained (in mM) 120 caesium methanesulphonate, 20 CsCl, 15 HEPES, 5 $MgCl_2$, 3 EGTA, pH adjusted to 7.3 with CsOH. To activate the TRPC3 channel, current cells were challenged with 100 μM carbachol or 100 μM 1-oleoyl-2-acetyl-*sn*-glycerol (OAG). For RBL-2H3 cells CRAC measurement, standard protocols and buffers were modified from Derler *et al.* (2009). In brief voltage ramps from –90 to +90 mV over 1 s (holding potential +30 mV) were applied and controlled by pClamp software. ECS contained (in mM) 130 NaCl, 5 CsCl, 1 $MgCl_2$, 10 HEPES, 10 glucose, 20 $CaCl_2$ at pH 7.4. ICS was comprised of 3.5 $MgCl_2$, 145 caesium methanesulphonate, 8 NaCl, 10 HEPES, 20 EGTA at pH 7.2. Experiments in HEK-293 cells expressing STIM1 and Orai1 to reconstitute the CRAC pore were done as in Muik *et al.* (2008). ECS contained (in mM) 145 NaCl, 5 CsCl, 1 $MgCl_2$, 10 HEPES, 10 Glucose, 10 $CaCl_2$ at pH 7.4. ICS was comprised of 3.5 $MgCl_2$, 145 caesium methanesulphonate, 8 NaCl, 10 HEPES, 20 EGTA at pH 7.2. For measuring the sodium currents in divalent-free conditions, protocols and buffers from Bergsmann *et al.* (2011) were used. If not mentioned otherwise for the experiments, cells were pre-incubated for 3 min and measured in the presence of either 3 μM Pyr2, Pyr3, Pyr6 or Pyr10.

Measurement of intercellular Ca^{2+}

Cells were loaded with 2 μM Fura-2-AM (Molecular Probes, LifeTechnologies, Vienna, Austria) for 45 min in Optimem® medium (Invitrogen) and washed. Cells were continuously perfused with Ca^{2+} free ECS buffer for any cell type as above and either challenged by depletion of intracellular Ca^{2+} stores with 1 μM thapsigargin (RBL-2H3) for 5 min, or by acute application of 100 μM carbachol (HEK293). Pyrazole compounds were supplied in corresponding concentration in the buffer at least 5 min before the start of the measurement. Agonists as well as inhibitors remained present continuously. For Ca^{2+} re-addition, 2 mM extracellular $CaCl_2$ was added. Excitation light was supplied via a Polychrome II polychromator (TILL Photonics, Gräfeling, Germany) and emission was detected by a Sensicam CCDcamera (PCO Computer Optics, Kelheim, Germany). Ca^{2+}-sensitive fluorescence ratios (340 nm/380 nm excitation; 510 nm emission) were recorded and analysed by using Axon Imaging Workbench (Axon Instruments).

NFAT translocation

For NFAT imaging experiments, coverslips with transfected RBL-2H3 cells were transferred into nominally Ca^{2+}-free RBL-2H3 buffer (described previously), and incubated with thapsigargin (1 μM) for 5 min to deplete the internal Ca^{2+} stores. NFAT translocation was triggered by adding 2 mM extracellular $CaCl_2$. Pyrazole compounds were present in all buffers at 10 μM. Basal NFAT localization was assessed from cells before store depletion.

GFP-NFAT translocation was monitored (488 nm laser excitation) with standard fluorescence microscopy (Zeiss Axiovert equipped with Coolsnap HQ, Zeiss, Oberkochen, Germany). Nuclear/cytosol fluorescence intensity ratios of cells were calculated with ImageJ software (Bethesda, MA, USA; http://imagej.nih.gov/ij/, 1997–2012). Nuclei were delineated in phase contrast images and visualized by DAPI staining. DAPI (AppliChem, Darmstadt, Germany) was used according to the manufacturer's recommendations on paraformaldehyde fixed cells.

Degranulation assay

Degranulation of RBL-2H3 cells was measured by determining the level of secreted β-hexosaminidase similar to Law *et al.* (2011). Cells were seeded out in 24-well plates and grown to confluency. All subsequent incubations were done at 37°C. After being washed with 2 mM $CaCl_2$ containing RBL-2H3 buffer (described previously), cells were incubated with either 3 or 10 μM pyrazole compounds for 15 min. Ionomycin was added to a final concentration of 0.4 μM per well and the incubation continued for a further 30 min. Aliquots (30 μL) of each well's supernatant were transferred to 96-well plates containing 50 μL of 1.3 $mg \cdot mL^{-1}$ p-nitrophenyl-n-acetyl-β-d-glucosaminide in 100 mM Na-citrate buffer (pH 4.5) as substrate. Aliquots of untreated and triton incubated (final concentration 2% triton, used in 1:10 dilution for substrate assay) cells were used as basal and maximal granula

content references. Control experiments were performed to test the potential interference of compounds with ionomycin function by elevating the ionomycin concentration 10-fold, which results in Ca^{2+} entry mediated mainly by direct Ca^{2+} transport via ionomycin pores in the plasma membrane. After 45 min, the enzymatic reaction was stopped with 50 µL 0.4 M glycine buffer (at pH 10.7). Absorbance was measured at 405 nm in a plate reader.

Drug target nomenclature, curve fitting, data evaluation and statistics

Nomenclature for drug targets conforms to BJP's Guide to Receptors and Channels (Alexander *et al.* 2011). Dose-response curves were fitted according a standard 4-parameter logistic equitation using Sigma Plot 12®. Data are presented as mean values ± SEM and were tested for statistical significance using one-way ANOVA in Sigma Plot® (Systat Software, Erkrath, Germany). *Indicates $P < 0.05$, **$P < 0.01$ and ***$P < 0.001$.

Results

Nomenclature and structure of pyrazole compounds

Pyrazole compounds were designated according to the previous literature and for novel structures following order of synthesis in our laboratory. Correct chemical nomenclature is Pyr2/BTP2 – *N*-(4-(3,5-bis(trifluoromethyl)-1*H*-pyrazole-1-yl)phenyl)-4-methyl-1,2,3-thiadiazole-5-carboxamide; Pyr3 – ethyl 1-(4-(2,3,3-trichloroacrylamido) phenyl)-5-(trifluoromethyl)-1*H*-pyrazole-4-carboxylate; Pyr6 – N-(4-(3,5-bis(trifluoromethyl)-1H-pyrazole-1-yl)phenyl)-3-fluoroisonicotinamide; Pyr10 – *N*-(4-(3,5-bis(trifluoromethyl)-1*H*-pyrazole-1-yl)phenyl)-4-methylbenzenesulfonamide (Obermayer *et al.*, 2011). As illustrated in Figure 1, Pyr2, Pyr6 and Pyr10 share the common backbone of BTPs with a trifluoromethyl-group on position C3 and C5 of the pyrazole ring, whereas Pyr3 lacks this at position C3 and is substituted with a carboxylate group on position C4 of the pyrazole ring. Estimating the octanol-water-coefficient (logP) of the four compounds by determining the hydro-/lipophilic behaviour revealed two groups: Pyr2, Pyr3 and Pyr6 (values 3.87, 3.89 and 3.84) versus Pyr10 with a higher value of 5.14. Calculation of the total molecular polar surface area as a second indicator of membrane permeability yielded 59.81 Å (Pyr6), 63.99 Å (Pyr10), 72.71 Å (Pyr2) and 73.23 Å (Pyr3), and did not suggest substantial differences in membrane permeability among these compounds.

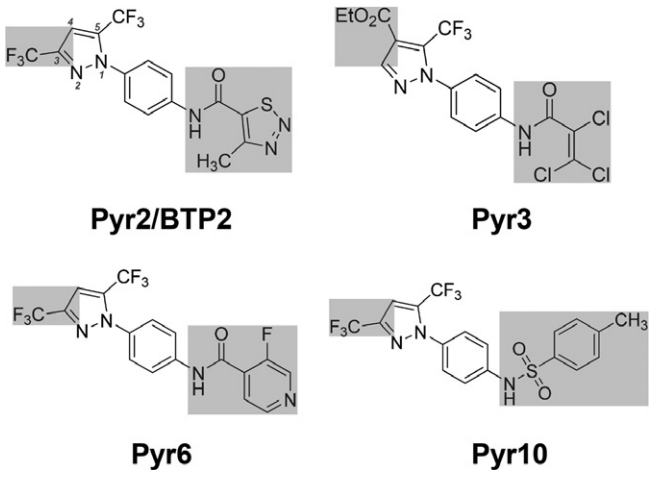

Figure 1

Chemical structures of the pyrazole compounds tested. Molecular structures suggested of importance for Ca^{2+} channel blocking activity are highlighted.

Potency and selectivity of pyrazole compounds in ROCE and SOCE model systems

The group of Mori reported a high selectivity of Pyr3 for TRPC3 channels as compared to channels formed by other TRPC species (Kiyonaka *et al.*, 2009). The potency and selectivity of this compound for classical SOCE, which was repeatedly suggested to overlap with TRPC signalling, has so far not been delineated. By contrast, another pyrazole, Pyr2 (BTP2), is commonly accepted as a pharmacological tool as well as an inhibitor of the classical SOCE pathways mediated by Orai1 (Zitt *et al.*, 2004). Here we set out to compare the TRPC/Orai1 selectivity of Pyr2 and Pyr3 along with Pyr6, and a newly synthesized structure designated as Pyr10 (Figure 1). The inhibitory potential of these four compounds on TRPC3-ROCE and SOCE was tested by measuring Ca^{2+} entry into stimulated cells using Fura-2 and classical Ca^{2+} re-addition protocols. As a ROCE model, HEK293 cells overexpressing YFP-tagged TRPC3, as a typical lipid/second messenger-controlled TRPC, were used. TRPC3 channels were activated by stimulating endogenous muscarinic receptors with 100 µM carbachol (Mundell and Benovic, 2000; Thyagarajan *et al.*, 2001). As a SOCE model native RBL-2H3 cells were employed, which display the prototypical STIM1/Orai1-mediated SOCE based on the classical CRAC conductance (Hoth and Penner, 1992; Calloway *et al.*, 2009). In this system, SOCE was activated by passively depleting the intracellular stores with thapsigargin before Ca^{2+} re-addition.

Table 1 and Figure 2 show the calculated IC_{50} values obtained from fitted dose-response curves. Notably, Pyr3

Table 1

IC_{50} of Ca^{2+} influx inhibition by pyrazoles in carbachol-stimulated YFP-TRPC3-transfected HEK293 cells for ROCE or thapsigargin-depleted native RBL-2H3 cells for SOCE

Pyrazole	$IC_{50\ (TRPC3\text{-}ROCE)}$ (µM)	$IC_{50\ (SOCE)}$ (µM)
Pyr2	4.21	0.59
Pyr3	0.54	0.54
Pyr6	18.46	0.49
Pyr10	0.72	13.08

Values were calculated by fitting the data shown in Figure 2 with a 4-parameter logistic function Data points were derived from 3–5 individual experiments and a total of 29–80 cells.

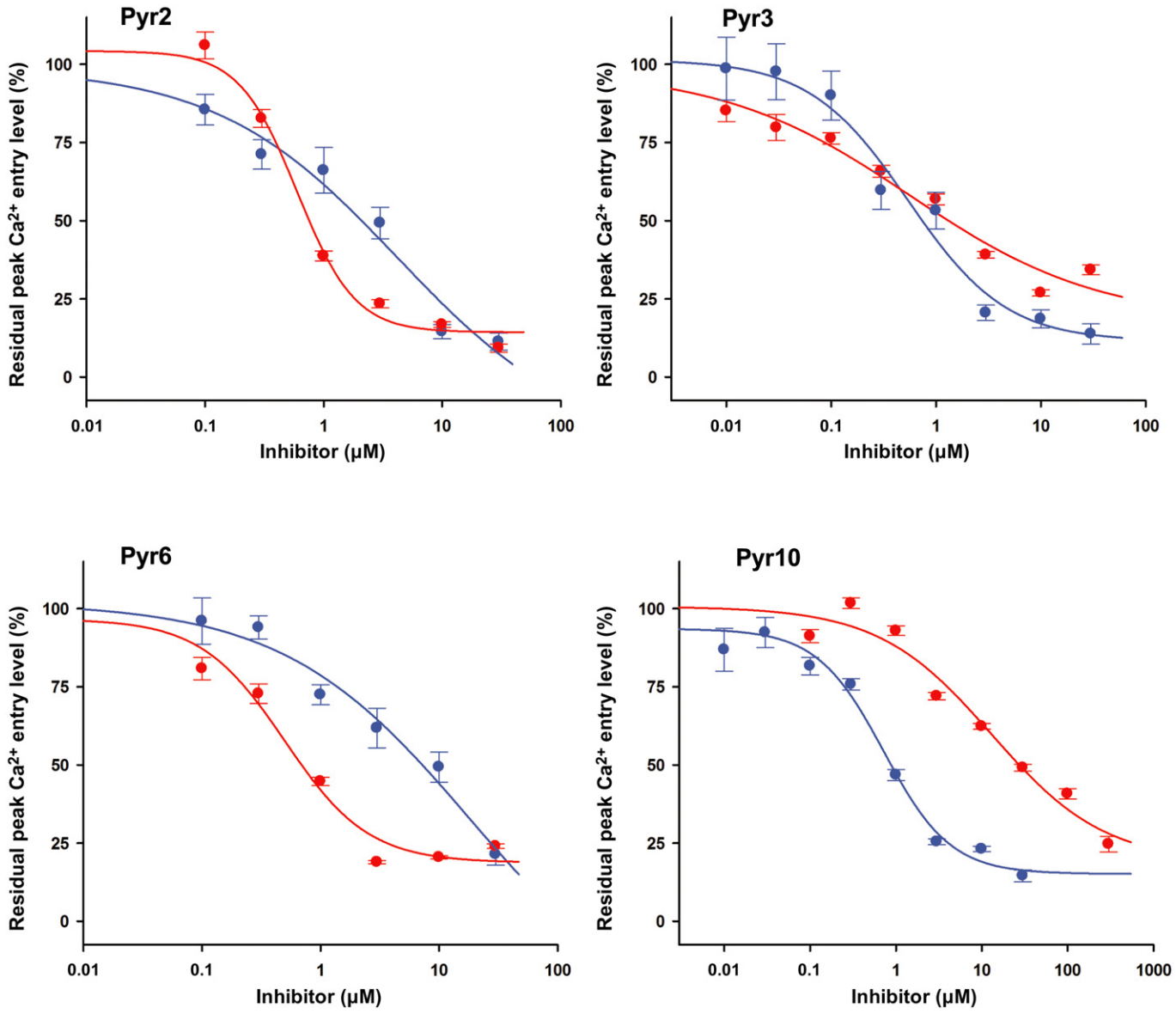

Figure 2

Concentration-dependence of Ca^{2+} entry inhibition by pyrazoles in TRPC3 overexpressing HEK293 cells and in native RBL-2H3 mast cells representing model systems of TRPC3-ROCE and SOCE. Fura-2 Ca^{2+} imaging experiments for YFP-TRPC3 transfected cells (ROCE model, blue symbols and line) or native RBL-2H3 (SOCE model, red symbols and line) and fitted dose-response curves. Inhibition is presented as percentage of the peak Ca^{2+} entry level measured in the absence of pyrazole compounds. Mean values ± SEM are given. Each value was derived from 3–5 individual experiments and a total of 29–80 cells. HEK293 YFP-TRPC3 cells were challenged with carbachol (100 μM) to stimulate ROCE. Native RBL-2H3 cells were incubated with thapsigargin (1 μM) before the experiment to elucidate SOCE by depleting intracellular Ca^{2+} stores.

lacked selectivity for TRPC3-ROCE in this test and displayed a similar potency for SOCE inhibition in native RBL-2H3 cells like Pyr2, which, in line with earlier reports, was found to be sevenfold [0.85 orders of magnitude (OM)] more potent in the SOCE than in the TRPC3-ROCE model (Sweeney *et al.*, 2009). Direct inhibition of the STIM1/Orai1-mediated CRAC currents was confirmed by reconstitution of the CRAC pore in HEK293 cells. Inhibition of CRAC elicited by passive store depletion using EGTA (10 mM) in the pipette solution, was observed upon acute administration in a rapid and dose-dependent manner. This effect was not readily reversed upon washout and was also evident in a divalent-free condition (Supporting Information Figure S1) representing monovalent permeation through CRAC channels (Hoth and Penner, 1993).

The most striking selectivity was obtained with Pyr6 and Pyr10. In line with earlier reports suggesting Pyr6 is a selective SOCE inhibitor (Yonetoku *et al.*, 2008; Sweeney *et al.*, 2009), Pyr6 displayed 37-fold (1.58 OM) higher potency for RBL SOCE than for TRPC3 ROCE, with an IC_{50} comparable to that

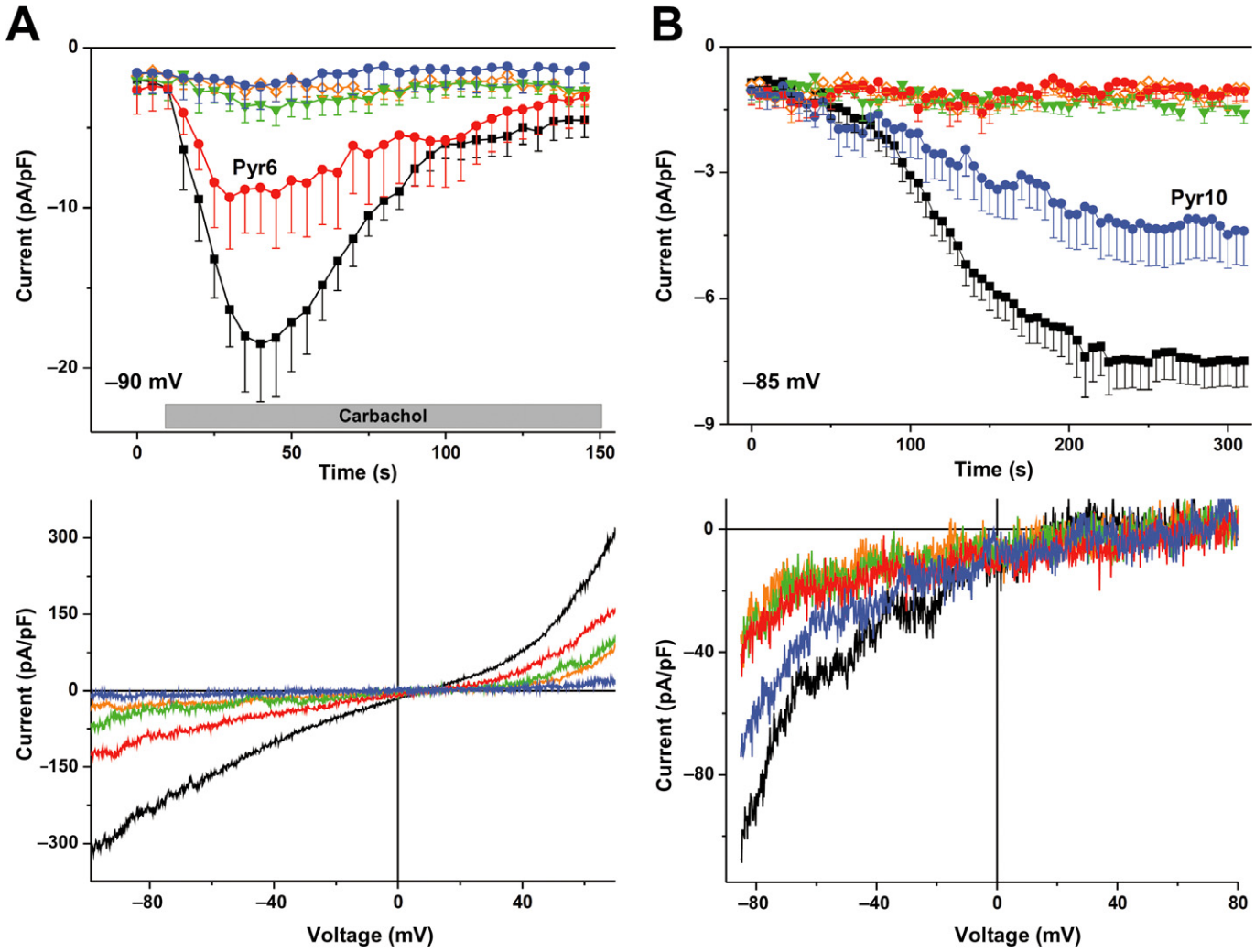

Figure 3

Differences in the selectivity of Pyr6 and Pyr10 for blocking TRPC3- and STIM1/Orai1-mediated membrane currents. (A) Top panel: time course of currents measured at –90 mv ($n \geq 7$ experiments for each condition) after incubation with pyrazoles for 5 min and stimulation of HEK-293 cells transiently expressing TRPC3 with carbachol (100 μM). Lower panel: representative *I-V* relationship of carbachol-stimulated currents in cells pretreated with pyrazole compound versus control. (B) Top panel: time course of CRAC currents in native RBL-2H3 cells after incubation with pyrazoles and store depletion with EGTA in the patch pipette ($n \geq 6$). Lower panel: representative *I-V* relationship of EGTA-induced currents in store-depleted RBL-2H3 cells, pretreated with pyrazole compound, versus control. Mean values ± SEM are given. In all experiments, pyrazoles were administrated at 3 μM concentrations. Symbols/colours: filled black square/black trace – untreated control; open orange square/orange trace – Pyr2; filled green triangle/green trace – Pyr3; filled red circle/red trace – Pyr6; filled blue circles/blue trace – Pyr10.

of Pyr2 and Pyr3. Interestingly, the sulphonamide-substituted compound Pyr10, by contrast, showed substantial selectivity for TRPC3-ROCE, being 18-fold (1.25 OM) more potent as compared with the SOCE model.

Pyr6 and Pyr10 – tools to distinguish between TRPC3 ROCE and STIM1/Orai1 SOCE

As Pyr6 and Pyr10 affected cellular Ca^{2+} handling in a divergent manner, we investigated their effects on TRPC and CRAC channels more directly by electrophysiology. In line with the Fura-2 imaging results, pre-incubation of cells with Pyr2 and Pyr3 at 3 μM completely eliminated the Ca^{2+} entry-mediating conductances in both cell types (Figure 3 and Table 2). In contrast, Pyr6 and Pyr10 interfered with these conductances in a selective manner. While completely inhibiting CRAC currents, Pyr6 at 3 μM diminished TRPC3 currents to only 52%. Pyr10 (3 μM) eliminated TRPC3 currents but suppressed SOCE in RBL-2H3 cells to only 60% of control. These results suggest Pyr6 and Pyr10 are potential tools for selectively affecting TRPC3 or Orai1 channels and demonstrate that Pyr3 clearly lacks selectivity. Inhibition of TRPC3 by Pyr10 was also observed when the channel was activated directly by the lipid mediator OAG (Supporting Information Fig. S2), demonstrating that this effect is not dependent on intracellular Ca^{2+} stores.

Table 2

Peak TRPC3-ROCE and SOCE currents in the absence and presence of 3 μM pyrazoles

Pyrazole	$I_{TRPC3\text{-}ROCE}$ (pA/pF)	Statistical significance	I_{SOCE} (pA/pF)	Statistical significance
Pyr2	−1.54 ± 0.53	*	−1.13 ± 0.16	***
Pyr3	−2.27 ± 0.96	*	−1.45 ± 0.19	***
Pyr6	−9.50 ± 2.66	n.a.	−1.31 ± 0.15	***
Pyr10	−1.01 ± 0.57	*	−4.49 ± 0.75	n.a.
no pyrazole	−18.50 ± 3.47	*	−7.50 ± 0.64	***

Currents were measured at maximal carbachol activation of ROCE in YFP-TRPC3-transfected HEK-293 cells or at −85 mV 300 s after perforating the cell for fully developed SOCE in native RBL-2H3 cells. Statistical significance was calculated compared with Pyr6-incubated cells for TRPC3-ROCE and compared with Pyr10 for SOCE. Values are mean values of net-currents (measured current minus basal current) ± SEM. (*$P < 0.05$, ***$P < 0.001$). n.a., not available.

Physiological consequences of Pyr-mediated inhibition of SOCE in RBL-2H3 cells

Due to the key role for Ca^{2+}, which acts as an important second messenger for transduction of plasma membrane signals to cellular functions including gene transcription, the effects of the four compounds on NFAT translocation and mast cell degranulation were examined. As shown in Figure 4A,B, SOCE inhibition by 10 μM Pyr2, Pyr3 or Pyr6 clearly inhibited NFAT translocation, whereas the selective TRPC3-ROCE inhibitor Pyr10 failed to suppress NFAT activation significantly.

The degranulation of RBL-2H3 initiated by ionomycin was inhibited by all the pyrazole compounds, with Pyr10 being the weakest inhibitor. The potent SOCE inhibitors Pyr2, Pyr3 and Pyr6 substantially reduced degranulation at 3 μM and suppressed responses down to basal levels at 10 μM, while Pyr10 (10 μM) prevented degranulation to only 65% of control. Therefore, these results clearly demonstrate that Orai1-mediated SOCE is a master regulator of degranulation and Ca^{2+}-dependent transcriptional control in RBL-2H3 cells but the TRPC permeation pathways do not significantly contribute to this process in these cells.

Discussion and conclusion

Pharmacological dissection of SOCE and ROCE pathways

In view of the currently incomplete understanding of the molecular structures involved in agonist/receptor-operated control of Ca^{2+} entry into many native tissues, it is highly desirable to identify potent inhibitors for specific Ca^{2+} channel pore structures that are controlled via receptor-phospholipase C-dependent mechanisms. A principal problem is the typical simultaneous activation of pathways activated by Ca^{2+} store depletion and by second messenger mechanisms such as generation or depletion of lipid mediators. These mechanisms not only overlap upon stimulation of PLC but may also both involve TRPC proteins as essential components (Putney, 2004). Nonetheless, pharmacological dissection of these mechanisms appears possible, based on different pore complexes of receptor/second messenger-operated and store-operated channels. Prototypical molecules mediating these Ca^{2+} entry mechanism are on the one hand TRPC3, which, upon overexpression, forms diacylglycerol-regulated non-selective cation channels and on the other hand Orai1, which forms a highly Ca^{2+} selective channel activated by interaction of the ER Ca^{2+} sensor STIM1 in response to a reduction in ER Ca^{2+} levels. Here we tested several potential blockers of TRPC and Orai channels for selectivity, including a recently synthesized, novel pyrazole compound termed Pyr10. We report the ability of two pyrazole compounds, Pyr6 and Pyr10, to discriminate between receptor-operated TRPC3 and native STIM1/Orai1 channels. At low micromolar concentrations, the novel structure Pyr10 completely eliminated TRPC3 currents as well as Ca^{2+} entry while exerting modest effects on Orai-mediated responses. Interestingly, CRAC currents displayed a somewhat higher sensitivity to Pyr10, as expected from Ca^{2+} entry measurements. Pyr10 (3 μM) inhibited CRAC currents by about 50%, while Ca^{2+} entry was reduced by only 30%. This difference could be based on the different experimental conditions, which to some extent affect channel regulation and may modulate drug sensitivity. Pyr6 displayed inverse selectivity, resulting in weak inhibition of TRPC3 currents at concentrations that eliminated Orai-mediated currents. Interestingly, the recently proposed TRPC3-selective blocker Pyr3 (Kiyonaka *et al.*, 2009), as well as Pyr2, a previously suggested inhibitor of store-operated Ca^{2+} entry and inhibitor of the classical CRAC current in immune cells, was barely able to distinguish between TRPC3 and Orai1 (Zitt *et al.*, 2004; He *et al.*, 2005; Kiyonaka *et al.*, 2009). Our current findings confirm the principle activity of pyrazole derivatives as inhibitors of CRAC currents and, thus, of Orai channels. For Pyr3, we found that this compound rapidly suppresses both native CRAC currents as well as heterologously reconstituted CRAC currents upon acute administration (Supporting Information Fig. S1A,B). The rapid inhibitory effect of Pyr3 observed upon extracellular administration may be interpreted as an interaction of the pyrazole with an extracellular target site at the Orai/CRAC channel complex. A similar conclusion was reached in a study characterizing the effects of Pyr2 on CRAC channels in T lymphocytes (Zitt *et al.*, 2004).

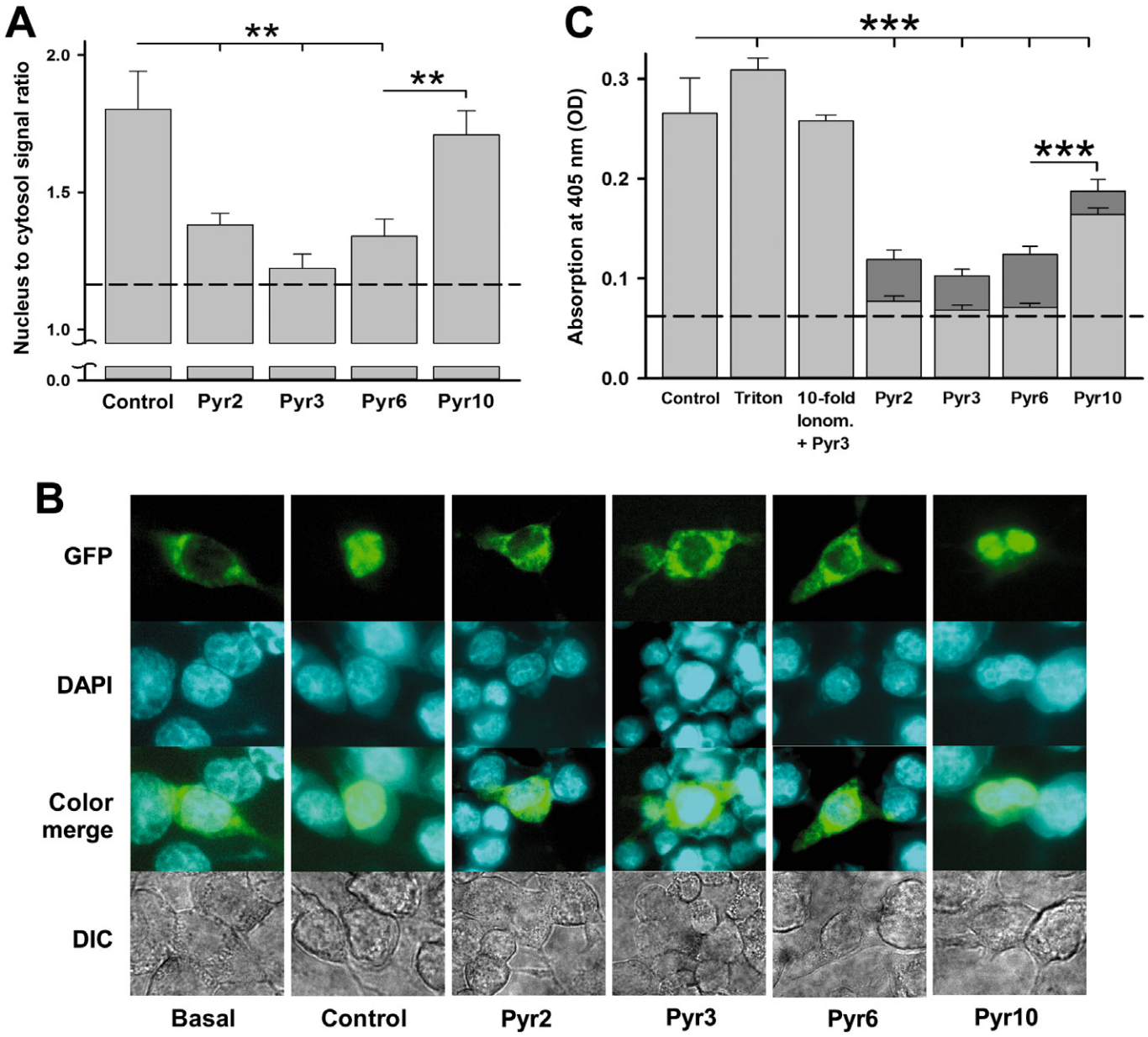

Figure 4

Pyrazol effects on NFAT activation and degranulation in RBL-2H3 cells. (A) Mean values ± SEM of NFAT nuclear to cytosolic ratio ($n \geq 18$ cells for each condition) Values were determined after depletion of intracellular Ca^{2+} stores with thapsigargin and re-addition of extracellular Ca^{2+} for control (thapsigargin only). Pyrazole-treated (10 μM) cells as indicated are compared with basal condition (dashed line). (B) Representative images of NFAT localization (GFP), localization of the nuclei (DAPI staining), an overlay of both and DIC microscopy images for basal, control and pyrazole-treated cells after paraformaldehyde fixation. (C) Mean values ± SEM of degranulation ($n = 3$ experiments from different passages) shown for control (ionomycin 0.4 μM only), for the effect of Pyr3 on cells stimulated by a 10-fold higher concentration of ionomycin (control for lack of interference of the pyrazole with ionomycin pore formation) and pyrazole-treated cells (3 μM – dark grey; 10 μM – light grey) stimulated with 0.4 μM ionomycin to initiate SOCE. Basal degranulation is indicated by a dashed line. Asterisks indicate statistical significant differences and refer to levels measured at 10 μM concentration of pyrazoles. (**$P < 0.01$, ***$P < 0.001$).

The observation that pyrazoles are able to inhibit CRAC channels after complete activation in response to store depletion, argues against suppression of the channel's activation process. Nonetheless, interference of the pyrazoles with inactivation or certain regulatory processes cannot be excluded at present. Consistent with inhibition of Orai channel activity, Pyr2, Pyr3 or Pyr6 substantially inhibited typical Orai downstream signalling events in RBL mast cells (NFAT activation and degranulation) activated by passive store depletion. Unequivocally, Pyr2 and Pyr3 also inhibit TRPC-mediated Ca^{2+} entry (He *et al.*, 2005; Kiyonaka *et al.*, 2009), and investigations performed in human neutrophils (Salmon and

Ahluwalia, 2010), pancreatic and salivary gland acinar cells (Kim *et al.*, 2011) demonstrated inhibition of SOCE by Pyr3, which was interpreted as a contribution of TRPC proteins to the SOCE phenomena (Salmon and Ahluwalia, 2011). However, insufficient selectivity of Pyr3 in terms of discrimination between TRPC and Orai channel pores as demonstrated here, weakens this conclusion.

The observed selectivity of Pyr6 and Pyr10 suggests that these compounds may be useful to identify and analyse TRPC- and Orai-mediated conductances in native tissues. Our results obtained in RBL-2H3 mast cells and STIM1/Orai1-expressing HEK293 cells were in line with the concept that store-operated Ca^{2+} entry in these two cell systems occurs via the same channels, which are characterized by sensitivity to Pyr6 being clearly higher than to Pyr10. By contrast, TRPC3 homomeric pore structures are highly sensitive to Pyr10 but weakly sensitive to Pyr6. Importantly, a test for inhibitory effects of Pyr6 and Pyr10 on homomeric channels of other TRPC isoforms such as TRPC4, 5 and 6, revealed a low potency (IC_{50} > 10 μM) at these channels, indicating that Pyr10 exhibits a significant TRPC subtype selectivity (Supporting Information Fig. S3).

We suggest a pyrazole sensitivity of Pyr6 > Pyr10 as a characteristic of Orai1-mediated Ca^{2+} entry. As RBL-2H3 cells express TRPC genes including TRPC3 (Ma *et al.*, 2008), our results may be taken as an indication that TRPC3 does not contribute to store-operated Ca^{2+} entry in mast cells. Nonetheless, we cannot exclude contribution of a TRPC3 containing channel complex in local Ca^{2+} signalling events that are not detectable as global cellular Ca^{2+} changes but could be pivotal for certain downstream signalling processes as recently reported for cardiac TRPC3s (Poteser *et al.*, 2011). Our finding of NFAT translocation being highly sensitivity to Pyr6 but not to Pyr10 is in line with the concept that in RBL-2H3 cells, NFAT is mainly controlled via the CRAC/Orai Ca^{2+} entry pathway, as recently suggested by Kar *et al.* (2011). It is of note that pyrazole structures have initially been recognized as effective inhibitors of NFAT signalling via an ill-defined mechanism downstream of Ca^{2+} signalling (Djuric *et al.*, 2000; Trevillyan *et al.*, 2001). Here we report that the inhibitory effects of Pyr6 and Pyr10 correlate well with their efficacy as CRAC/Orai1 inhibitors. The observation that Pyr6 was more potent than Pyr10 as a suppressant of mast cell degranulation corroborates the view that Orai channels represent the main source of Ca^{2+} for exocytosis in RBL-2H3 cells (Ma *et al.*, 2008). Consistent with previous reports, Pyr6 was found to be highly effective as an inhibitor of immune cell transcriptional activation and cytokine production (Ishikawa *et al.*, 2003; Birsan *et al.*, 2004; Shirakawa *et al.*, 2010; Law *et al.*, 2011), underscoring the potential value of this chemical structure for the development of potent immune modulators (Chen *et al.*, 2002; Zitt *et al.*, 2004).

Structural basis of selective modulation of Ca^{2+} signalling by pyrazoles

The structural basis of Ca^{2+} entry block by pyrazoles has recently been analysed. The C3 position in the pyrazole ring was recognized as a critical determinant of the inhibitory effects on mast cell degranulation, most likely corresponding to inhibition of SOCE. Block of SOCE apparently requires substitution with bulky, electron-drawing groups in C3. However, a similar substitution in C5, as present in Pyr3, by itself was found to be insufficient to provide SOCE blocking activity. (Law *et al.*, 2011) Our finding of a high SOCE inhibiting potency of Pyr3 indicates that the introduction of an ethyl-carboxylate in C4 of Pyr3 restores inhibitory potency, although appropriate C3 substitution is lacking. Interestingly, substitution in C4 was suggested of importance for the Pyr3 potency regarding inhibition of TRPC family members (Kiyonaka *et al.*, 2009). Moreover, this later study also proposed the amid-bond linked side-group as pivotal for TRPC subtype selectivity, with the tricholoraryl-substitution in Pyr3 as the TRPC3 selectivity encompassing structural element. This amid-bond linked side group is, according to our results, also a potential structural determinant for the CRAC/SOCE inhibitory action, as this structural feature is lacking in the weak SOCE inhibitor Pyr10. Notably, Pyr10 contains a sulphonamide-linked side-group at the BTP backbone. One might speculate about substantial changes within the molecule generated by different interactions between the backbone and the side-group resulting in structures that discriminate between the two channel types. As electronegativity and polarity of the amine-linked side groups in Pyr3 and Pyr10 are similar, it is tempting to speculate that these structures are essential for inhibition of TRPC3-ROCE with high potency. Although a direct interaction of pyrazoles with TRPC3, presumably involving association to an extracellular binding domain, appears likely and has been demonstrated for Pyr3 (Kiyonaka *et al.*, 2009), the exact molecular basis of pyrazole action at the TRPC channel remains to be elucidated.

In this study, we obtained evidence for a possible value of pyrazoles as selective modulators of cellular Ca^{2+} handling, widening the view on both their therapeutic potential as immunosuppressants as well as their utility for experimental dissection of Ca^{2+} signalling pathways. In aggregate, we introduce a novel pharmacological approach to distinguish between second messenger-gated TRPC-mediated and store-operated, Orai-mediated Ca^{2+} entry using selective pyrazole compounds including Pyr10 as a novel TRPC3-selective inhibitor. The identified ability of certain pyrazole structures to discriminate between a receptor- and store-operated Ca^{2+} signalling pathway is expected to pave the way towards both better experimental analysis and understanding of Ca^{2+} entry mechanisms in native tissues and for the development of novel therapeutic strategies.

Acknowledgements

This work was funded by FWF (Austrian research fund) projects P21925-B19 (to K G), P22565-B18 (to C R) and the DK+ Metabolic and Cardiovascular Disease grant W1226-B18. We like to thank Renate Schmidt and Ines Neubacher for their technical assistance, Sonia Stürmer for support with preliminary experiments, as well as RH Kehlenbach and M Zhu for kindly providing the GFP-NFAT and GFP-TRPC6 construct.

Conflict of interest

The authors declare no conflict of interest.

References

Abramowitz J, Birnbaumer L (2009). Physiology and pathophysiology of canonical transient receptor potential channels. FASEB J 23: 297–328.

Alexander SP, Mathie A, Peters JA (2011). Guide to receptors and channels (GRAC), 5th edition. Br J Pharmacol 164 (Suppl. 1): S1–324.

Bergsmann J, Derler I, Muik M, Frischauf I, Fahrner M, Pollheimer P *et al.* (2011). Molecular determinants within N terminus of Orai3 protein that control channel activation and gating. J Biol Chem 286: 31565–31575.

Berridge MJ, Lipp P, Bootman MD (2000). The versatility and universality of calcium signalling. Nat Rev Mol Cell Biol 1: 11–21.

Birsan T, Dambrin C, Marsh KC, Jacobsen W, Djuric SW, Mollison KW *et al.* (2004). Preliminary in vivo pharmacokinetic and pharmacodynamic evaluation of a novel calcineurin-independent inhibitor of NFAT. Transpl Int 17: 145–150.

Calloway N, Vig M, Kinet JP, Holowka D, Baird B (2009). Molecular clustering of STIM1 with Orai1/CRACM1 at the plasma membrane depends dynamically on depletion of Ca2+ stores and on electrostatic interactions. Mol Biol Cell 20: 389–399.

Chen Y, Smith ML, Chiou GX, Ballaron S, Sheets MP, Gubbins E *et al.* (2002). TH1 and TH2 cytokine inhibition by 3,5-bis(trifluoromethyl)pyrazoles, a novel class of immunomodulators. Cell Immunol 220: 134–142.

Cheng KT, Liu X, Ong HL, Swaim W, Ambudkar IS (2011). Local Ca(2)+ entry via Orai1 regulates plasma membrane recruitment of TRPC1 and controls cytosolic Ca(2)+ signals required for specific cell functions. PLoS Biol 9: e1001025.

DeHaven WI, Smyth JT, Boyles RR, Bird GS, Putney JW, Jr (2008). Complex actions of 2-aminoethyldiphenyl borate on store-operated calcium entry. J Biol Chem 283: 19265–19273.

Derler I, Fahrner M, Carugo O, Muik M, Bergsmann J, Schindl R *et al.* (2009). Increased hydrophobicity at the N terminus/membrane interface impairs gating of the severe combined immunodeficiency-related ORAI1 mutant. J Biol Chem 284: 15903–15915.

Di Capite J, Parekh AB (2009). CRAC channels and Ca2+ signaling in mast cells. Immunol Rev 231: 45–58.

Djuric SW, BaMaung NY, Basha A, Liu H, Luly JR, Madar DJ *et al.* (2000). 3,5-Bis(trifluoromethyl)pyrazoles: a novel class of NFAT transcription factor regulator. J Med Chem 43: 2975–2981.

Glasnov TN, Groschner K, Kappe CO (2009). High-speed microwave-assisted synthesis of the trifluoromethylpyrazol-derived canonical transient receptor potential (TRPC) channel inhibitor Pyr3. ChemMedChem 4: 1816–1818.

Graziani A, Poteser M, Heupel WM, Schleifer H, Krenn M, Drenckhahn D *et al.* (2010). Cell-cell contact formation governs Ca2+ signaling by TRPC4 in the vascular endothelium: evidence for a regulatory TRPC4-beta-catenin interaction. J Biol Chem 285: 4213–4223.

Harteneck C, Gollasch M (2011). Pharmacological modulation of diacylglycerol-sensitive TRPC3/6/7 channels. Curr Pharm Biotechnol 12: 35–41.

He LP, Hewavitharana T, Soboloff J, Spassova MA, Gill DL (2005). A functional link between store-operated and TRPC channels revealed by the 3,5-bis(trifluoromethyl)pyrazole derivative, BTP2. J Biol Chem 280: 10997–11006.

Hofmann T, Obukhov AG, Schaefer M, Harteneck C, Gudermann T, Schultz G (1999). Direct activation of human TRPC6 and TRPC3 channels by diacylglycerol. Nature 397: 259–263.

Hoth M, Penner R (1992). Depletion of intracellular calcium stores activates a calcium current in mast cells. Nature 355: 353–356.

Hoth M, Penner R (1993). Calcium release-activated calcium current in rat mast cells. J Physiol 465: 359–386.

Ishikawa J, Ohga K, Yoshino T, Takezawa R, Ichikawa A, Kubota H *et al.* (2003). A pyrazole derivative, YM-58483, potently inhibits store-operated sustained Ca2+ influx and IL-2 production in T lymphocytes. J Immunol 170: 4441–4449.

Jardin I, Lopez JJ, Salido GM, Rosado JA (2008). Orai1 mediates the interaction between STIM1 and hTRPC1 and regulates the mode of activation of hTRPC1-forming Ca2+ channels. J Biol Chem 283: 25296–25304.

Kar P, Nelson C, Parekh AB (2011). Selective activation of the transcription factor NFAT1 by calcium microdomains near Ca2+ release-activated Ca2+ (CRAC) channels. J Biol Chem 286: 14795–14803.

Kim MS, Lee KP, Yang D, Shin DM, Abramowitz J, Kiyonaka S *et al.* (2011). Genetic and pharmacologic inhibition of the Ca2+ influx channel TRPC3 protects secretory epithelia from Ca2+-dependent toxicity. Gastroenterology 140: 2107–2115. 2115 e2101-2104.

Kiyonaka S, Kato K, Nishida M, Mio K, Numaga T, Sawaguchi Y *et al.* (2009). Selective and direct inhibition of TRPC3 channels underlies biological activities of a pyrazole compound. Proc Natl Acad Sci USA 106: 5400–5405.

Law M, Morales JL, Mottram LF, Iyer A, Peterson BR, August A (2011). Structural requirements for the inhibition of calcium mobilization and mast cell activation by the pyrazole derivative BTP2. Int J Biochem Cell Biol 43: 1228–1239.

Lemonnier L, Trebak M, Putney JW, Jr (2008). Complex regulation of the TRPC3, 6 and 7 channel subfamily by diacylglycerol and phosphatidylinositol-4,5-bisphosphate. Cell Calcium 43: 506–514.

Liao Y, Erxleben C, Yildirim E, Abramowitz J, Armstrong DL, Birnbaumer L (2007). Orai proteins interact with TRPC channels and confer responsiveness to store depletion. Proc Natl Acad Sci USA 104: 4682–4687.

Ma HT, Peng Z, Hiragun T, Iwaki S, Gilfillan AM, Beaven MA (2008). Canonical transient receptor potential 5 channel in conjunction with Orai1 and STIM1 allows Sr2+ entry, optimal influx of Ca2+, and degranulation in a rat mast cell line. J Immunol 180: 2233–2239.

Muik M, Frischauf I, Derler I, Fahrner M, Bergsmann J, Eder P *et al.* (2008). Dynamic coupling of the putative coiled-coil domain of ORAI1 with STIM1 mediates ORAI1 channel activation. J Biol Chem 283: 8014–8022.

Mundell SJ, Benovic JL (2000). Selective regulation of endogenous G protein-coupled receptors by arrestins in HEK293 cells. J Biol Chem 275: 12900–12908.

Ng SW, di Capite J, Singaravelu K, Parekh AB (2008). Sustained activation of the tyrosine kinase Syk by antigen in mast cells requires local Ca2+ influx through Ca2+ release-activated Ca2+ channels. J Biol Chem 283: 31348–31355.

Nilius B, Owsianik G, Voets T, Peters JA (2007). Transient receptor potential cation channels in disease. Physiol Rev 87: 165–217.

Obermayer D, Glasnov TN, Kappe CO (2011). Microwave-assisted and continuous flow multistep synthesis of 4-(pyrazol-1-yl)carboxanilides. J Org Chem 76: 6657–6669.

Pedersen SF, Owsianik G, Nilius B (2005). TRP channels: an overview. Cell Calcium 38: 233–252.

Poteser M, Schleifer H, Lichtenegger M, Schernthaner M, Stockner T, Kappe CO *et al.* (2011). PKC-dependent coupling of calcium permeation through transient receptor potential canonical 3 (TRPC3) to calcineurin signaling in HL-1 myocytes. Proc Natl Acad Sci USA 108: 10556–10561.

Prakriya M, Feske S, Gwack Y, Srikanth S, Rao A, Hogan PG (2006). Orai1 is an essential pore subunit of the CRAC channel. Nature 443: 230–233.

Putney JW, Jr (2004). The enigmatic TRPCs: multifunctional cation channels. Trends Cell Biol 14: 282–286.

Salmon MD, Ahluwalia J (2010). Discrimination between receptor- and store-operated Ca(2+) influx in human neutrophils. Cell Immunol 265: 1–5.

Salmon MD, Ahluwalia J (2011). Pharmacology of receptor operated calcium entry in human neutrophils. Int Immunopharmacol 11: 145–148.

Schindl R, Frischauf I, Kahr H, Fritsch R, Krenn M, Derndl A *et al.* (2008). The first ankyrin-like repeat is the minimum indispensable key structure for functional assembly of homo- and heteromeric TRPC4/TRPC5 channels. Cell Calcium 43: 260–269.

Shirakawa H, Sakimoto S, Nakao K, Sugishita A, Konno M, Iida S *et al.* (2010). Transient receptor potential canonical 3 (TRPC3) mediates thrombin-induced astrocyte activation and upregulates its own expression in cortical astrocytes. J Neurosci 30: 13116–13129.

Sinkins WG, Goel M, Estacion M, Schilling WP (2004). Association of immunophilins with mammalian TRPC channels. J Biol Chem 279: 34521–34529.

Sweeney ZK, Minatti A, Button DC, Patrick S (2009). Small-molecule inhibitors of store-operated calcium entry. ChemMedChem 4: 706–718.

Thyagarajan B, Poteser M, Romanin C, Kahr H, Zhu MX, Groschner K (2001). Expression of Trp3 determines sensitivity of capacitative Ca2+ entry to nitric oxide and mitochondrial Ca2+ handling: evidence for a role of Trp3 as a subunit of capacitative Ca2+ entry channels. J Biol Chem 276: 48149–48158.

Trebak M, Bird GS, McKay RR, Putney JW, Jr (2002). Comparison of human TRPC3 channels in receptor-activated and store-operated modes. Differential sensitivity to channel blockers suggests fundamental differences in channel composition. J Biol Chem 277: 21617–21623.

Trevillyan JM, Chiou XG, Chen YW, Ballaron SJ, Sheets MP, Smith ML *et al.* (2001). Potent inhibition of NFAT activation and T cell cytokine production by novel low molecular weight pyrazole compounds. J Biol Chem 276: 48118–48126.

Woodard GE, Lopez JJ, Jardin I, Salido GM, Rosado JA (2010). TRPC3 regulates agonist-stimulated Ca2+ mobilization by mediating the interaction between type I inositol 1,4,5-trisphosphate receptor, RACK1, and Orai1. J Biol Chem 285: 8045–8053.

Yonetoku Y, Kubota H, Miyazaki Y, Okamoto Y, Funatsu M, Yoshimura-Ishikawa N *et al.* (2008). Novel potent and selective Ca2+ release-activated Ca2+ (CRAC) channel inhibitors. Part 3: synthesis and CRAC channel inhibitory activity of 4′-[(trifluoromethyl)pyrazol-1-yl]carboxanilides. Bioorg Med Chem 16: 9457–9466.

Yuan JP, Kim MS, Zeng W, Shin DM, Huang G, Worley PF *et al.* (2009). TRPC channels as STIM1-regulated SOCs. Channels (Austin) 3: 221–225.

Zhang SL, Yu Y, Roos J, Kozak JA, Deerinck TJ, Ellisman MH *et al.* (2005). STIM1 is a Ca2+ sensor that activates CRAC channels and migrates from the Ca2+ store to the plasma membrane. Nature 437: 902–905.

Zitt C, Strauss B, Schwarz EC, Spaeth N, Rast G, Hatzelmann A *et al.* (2004). Potent inhibition of Ca2+ release-activated Ca2+ channels and T-lymphocyte activation by the pyrazole derivative BTP2. J Biol Chem 279: 12427–12437.

Supporting information

Additional Supporting Information may be found in the online version of this article:

Figure S1 Pyr3 acutely blocks a reconstituted CRAC pore in a dose-dependent, non-reversible manner as well as affecting sodium influx through it. (A) Time course of measured currents (n = 4 cells) of acute Pyr3 inhibition of CRAC in a HEK293 cell system expressing STIM1 and Orai1 to reconstitute the CRAC pore. (B) Time course of acute Pyr3 inhibition (3μM) in native RBL-2H3 cells (n = 6 cells). (C) Time course of currents (n = 8 cells) with acute Pyr3 inhibition of a reconstituted CRAC pore. Pyrazole compound was applied for only a limited time to examine reversibility of inhibitory effect. (D) Time course of Pyr3-effect (10 μM) on divalent-free sodium current through CRAC-pore after activation of current in Ca^{2+} containing buffer (n = 4 cells). All values are mean values ± SEM.

Figure S2 Pyr10 potently blocks DAG-mediated TRPC3 membrane currents. Mean values of OAG-induced (100 μM) TRPC3 currents in HEK293 cells in the absence and presence of 3 μM Pyr10. Mean values ± SEM of (n = 6).

Figure S3 Selectivity of Pyr10 and Pyr6 on TRPCs. Average inhibition of peak calcium entry level measured by Fura 2 Ca^{2+} imaging at 10 μM Pyr6 or Pyr10 in HEK293 cells overexpressing TRPC4beta-YFP, YFP-TRPC5 or GFP-TRPC6. HEK293 cells were challenged with carbachol (100 μM) to stimulate calcium entry and pre-incubated for 5 min with corresponding pyrazole compounds. Values are presented as percentage of non-inhibited carbachol-stimulated cells from the same experiments and were derived from a total of 27–55 cells from three individual experiments.